MICHIGAN STATE UNIVERSITY

CYCLOTRON LABORATORY

MICROSCOPIC ANALYSIS OF "MACROSCOPIC" EFFECTS IN RELATIVISTIC HEAVY ION COLLISIONS - TOWARDS THE NUCLEAR MATTER EQUATION OF STATE

JOSEPH J. MOLITORIS AND HORST STÖCKER

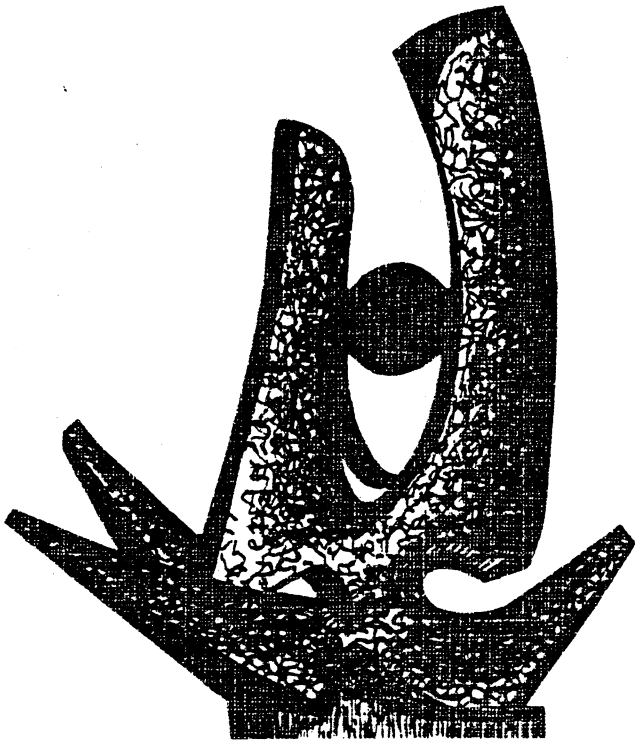

DECEMBER 1984

MSUCL-498

MSUCL-498
December 1984

Microscopic Analysis of "Macroscopic" Effects in Relativistic Heavy Ion Collisions - Towards the Nuclear Matter Equation of State

Joseph J. Molitoris and Horst Stöcker

National Superconducting Cyclotron Laboratory and
Department of Physics and Astronomy,
Michigan State University, East Lansing, Michigan 48824

Abstract

Recent high multiplicity selected 4π data on collective flow and pion production from the GSI-LBL Plastic Ball and Streamer Chamber collaborations have yielded qualitatively new results which could not be understood on the basis of microscopic simulations such as the intranuclear cascade model. We present evidence that this is due to the neglect of the repulsive many body interactions in the dense nuclear medium. Results of a variety of microscopic calculations which include a nuclear matter equation of state (the classical equation of motion simulations, the Vlasov Uehling-Uhlenbeck theory, and the time dependent Dirac equation with meson field dynamics as well as the macroscopic nuclear fluid dynamical model) as well as their

One of the most important open problems for relativistic heavy ion physics concerns the extraction of the nuclear matter equation of state. How can the yields and the emission pattern of the reaction products be used to extract information on the early hot and compressed stage of the collision? One of the first predicted signatures for nuclear stopping and compression is the sidewards flow of nuclear matter in head-on collisions of massive equal nuclei[1] (see Fig. 1). In contrast to the density and temperature, which first increase, but then steadily decrease during the course of the collision, the predominant emission pattern is established at the time of highest compression (i.e. at the highest pressure) and stays constant during the expansion. Pion and entropy production exhibit the same time dependence; hence they can also yield information on the high density stage of the reaction. One may view the flow as a barometer, the pion yield as a calorimeter, and the entropy as a measure for the number of degrees of freedom for high density matter.

In this paper we give a survey of recent experimental and theoretical developments in the field of high energy heavy ion reactions. First we give an overview of the various theoretical approaches developed to describe the complicated collision dynamics, discussing also the recent 4π experiments on pion production and flow. Next we discuss the status of recent attempts to determine the entropy from light and medium mass fragment abundancies. Finally, we turn to the high energy domain, $E_{Lab} >> 1$ GeV/N. We discuss the deconfinement phase transition from hadron matter into the quark gluon plasma, with particular emphasis on the available energy densities, the transition parameters and the space time structure of the high energy density regions.

Preferential sidewards emission of fragments from central collisions of high energy nuclei had been reported previously for very asymmetric reactions, e.g. C + Ag and Ne + U: early particle track detector experiments[2] yielded peaks in the angular distribution of alpha particles emitted from central C+Ag reactions, and the double differential cross sections of light fragments (p,d,t) emitted from high multiplicity selected collisions of Ne (393 MeV/n) + U exhibit sidewards maxima,[3] in accord with predictions of the fluid dynamical model.[4]

Recently it has been proposed to observe the collective flow directly via a kinetic energy flow analysis[5,6] on an event-by-event basis. The sensitivity[6] of the flow analysis for very heavy systems to the properties of nuclear matter at high densities and excitation energies is particularly fascinating. The basic idea of the flow analysis is to measure event-by-event the momenta of all (charged) particles. Such an analysis can be done experimentally only with 4π detector systems such as emulsion, streamer chamber, or the plastic ball. Once this information is available, the momenta are transformed into the center-of-momentum frame and the direction of the maximum kinetic energy flow is determined by performing a principal axis transformation.

The kinetic energy flow tensor K_{ij},

$$K_{ij} = \sum_{\nu} \frac{p_i(\nu)\, p_j(\nu)}{2 \quad m(\nu)} \quad , \qquad (1)$$

insures that composite fragments ν contribute to the matter flow tensor with the correct weight relative to nucleons.[5-7] For the reaction ^{93}Nb (E_{lab} =

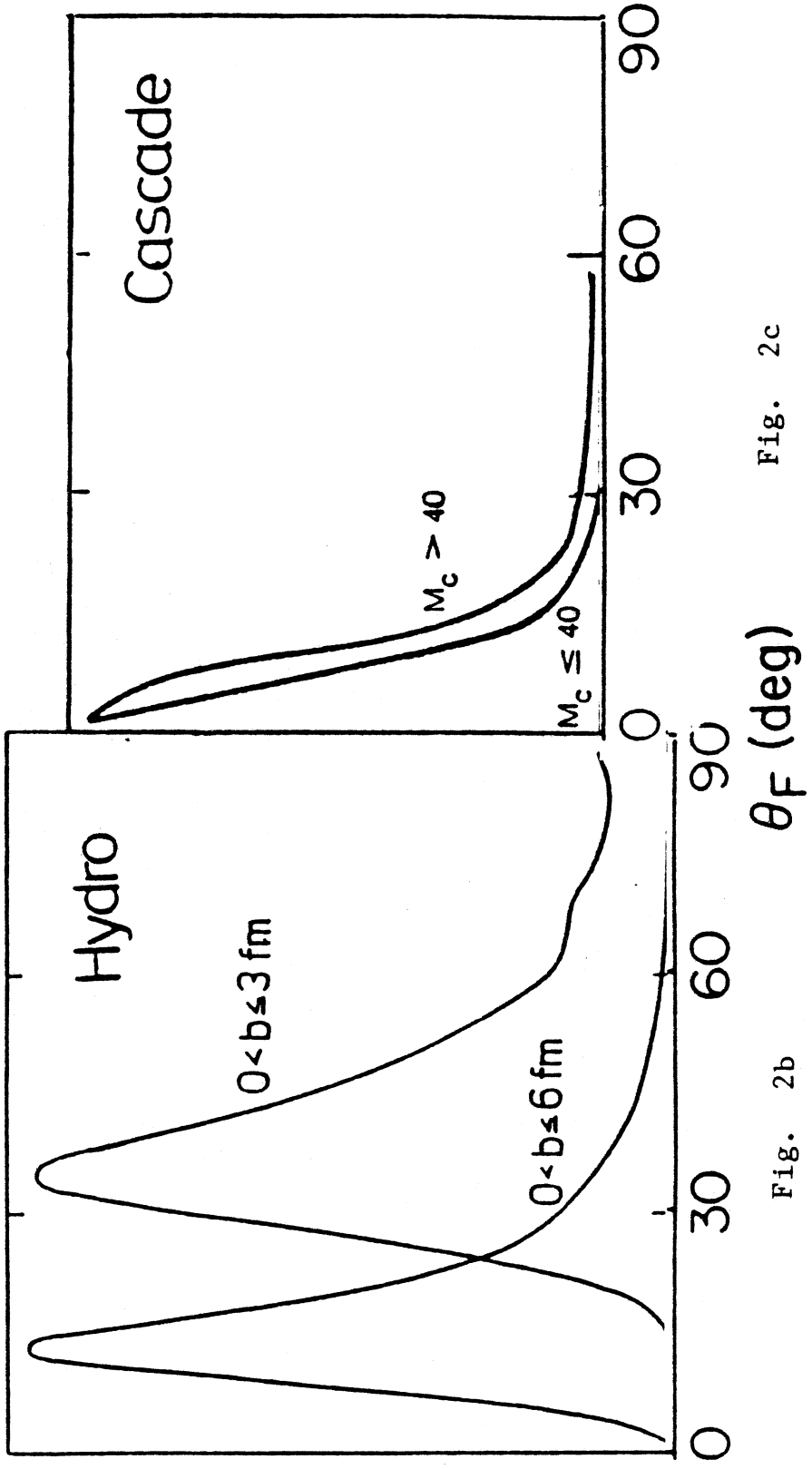
Hydro
0<b≤3 fm
0<b≤6 fm
Cascade
$M_c > 40$
$M_c \leq 40$
0
30
60
90
θ_F (deg)
$dN/d\cos\theta_F$ (arb. units)

Fig. 2b

Fig. 2c

momenta consistent with experimental values which results in an average binding energy of 7 MeV/N.

To simulate a collision process, the nuclei are Galilei-boosted with the respective center of mass momenta at given impact parameter. The equations of motion are integrated numerically. The evolution of a collision at b = 3 fm impact parameter is shown in Fig 1. The resulting sidewards flow can clearly be seen. The individual collisions are analyzed by diagonalizing the kinetic energy flow tensor. The distribution of flow angles $dN/d\cos\theta_F$ is presented in Fig. 2d for two impact parameter intervals. The qualitative and quantitative behavior of the flow pattern in the EOM model is very similar to the behaviour observed previously in hydrodynamics:[13] the flow angle θ_F rises smoothly from 0° at large impact parameters to 90° at b=0. A finite range of impact parameters is sampled to compute the angular distributions of the flow angles, $dN/d\cos\theta_F$. The distribution of flow angles is computed by taking into account the formation of fragments via a 6-dimensinal coalescence model recently developed.[14] We find roughly the same flow distribution by doing the flow analysis with and without clustering.

This model predicts peaks in the angular distribution of the flow angles which shift to larger angles with increasing multiplicity in agreement with the data. The physical difference between the INC model and the EOM approach, which leads to such distinct predictions, can be traced back to the different treatments of the NN collision process. The INC applies a stochastic 4π scattering at the point of closest approach of straight line trajectories; this allows for substantial transparency. In contrast, the repulsive short range component in the NN potential is a hard core and thus results in an excluded volume effect; thus the nuclei are not

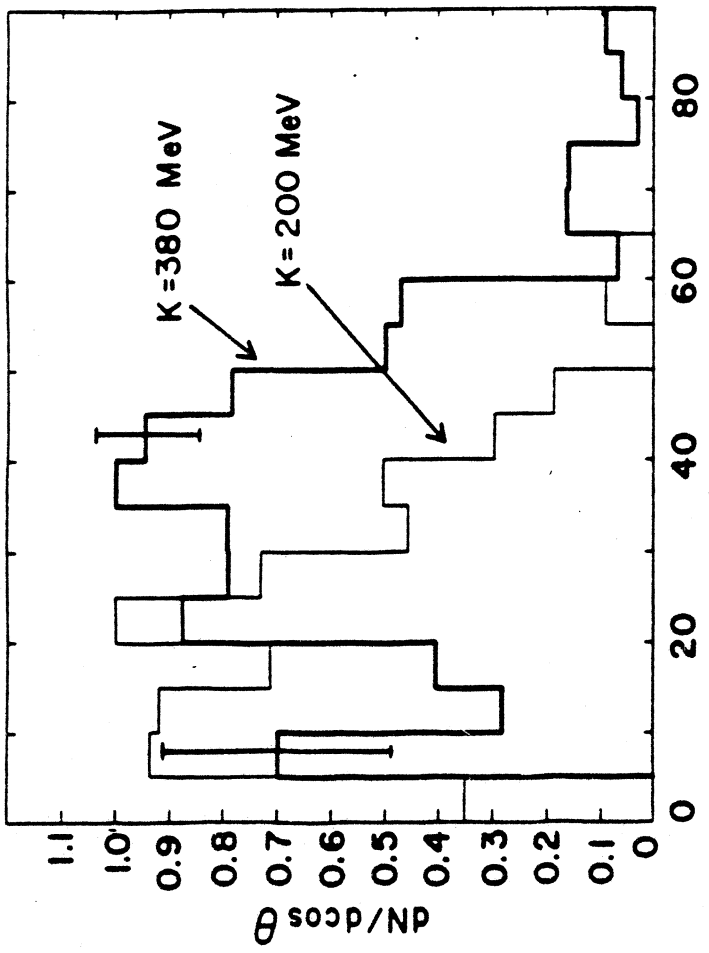
K=380 MeV
K=200 MeV
dN/dcos θ
THETA (DEGREES)

Fig. 3a

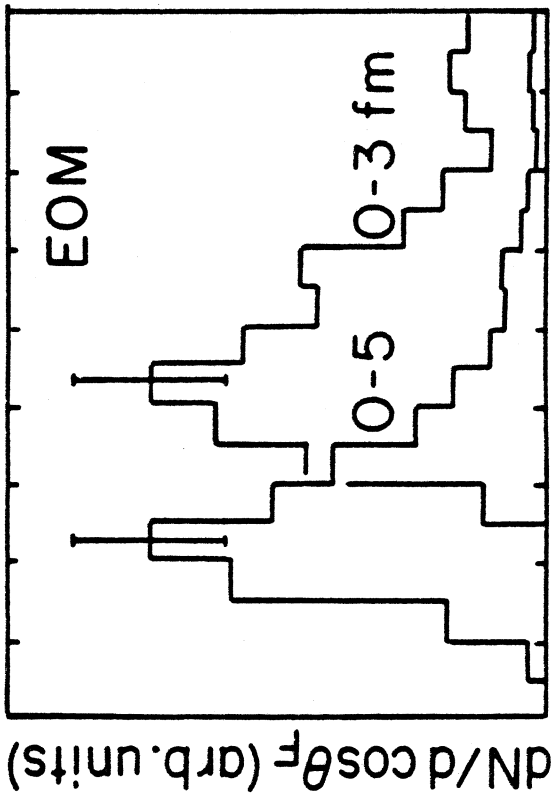
EOM
0-5
0-3 fm
dN/d cosθ_F (arb. units)
THETA (DEGREES)

Fig. 2d

Fig. 2b shows the distribution of flow angles, $dN/d\cos\theta_F$. The theoretically obtained[13] high multiplicity triggered events, corresponding to the small impact parameters (b=0 to 3 fm) compare favorably with the high multiplicity selected experimental data. The intermediate multiplicities ($30 < M < 40$) correspond to larger impact parameters, $3 < b < 6$ fm in the hydrodynamical calculation. The experimentally observed decrease of the average flow angle (by $\theta_F = 15°$) is well reproduced by the fluid dynamical calculation.

4. The Vlasov Equation with Uehling Uhlenbeck's Collision Term

This theory explains for the first time simultaneously both the observed collective flow and the pion multiplicity and gives their dependence on the nuclear equation of state in a microscopic approach.[14] Vlasov's equation for the evolution of the single particle distribution function f of a collisionless plasma in a self- consistent mean potential field is supplemented by Uehling- Uhlenbeck's quantum mechanical extension of Boltzmann's two body collision term which respects the Pauli principle (acronym VUU). This extended Boltzmann equation can be written[14,16,17]

$$\frac{\partial}{\partial t} f + \vec{v} \cdot \frac{\partial}{\partial \vec{r}} f - \frac{1}{m} \frac{\partial}{\partial \vec{r}} U(n) \cdot \frac{\partial}{\partial \vec{v}} f = \int \frac{d^3p_2 d^3p_1' d^3p_2'}{(2\pi)^6} \sigma v_{12} \times$$

$$\times \left[ff_2(1-f_1')(1-f_2') - f_1'f_2'(1-f)(1-f_2)\right]\delta^3(p+p_2-p_1'-p_2'). \qquad (4)$$

The Vlasov equation is solved by simultaneous numerical integration of the classical equations of motion of 15 parallel ensembles of $A_P + A_T$ test particles, which are initially assigned Fermi momenta and random positions in a sphere of nuclear radius. Two test particles from a given ensemble may undergo s-wave scattering if they approach each other within a distance $d^2 =$

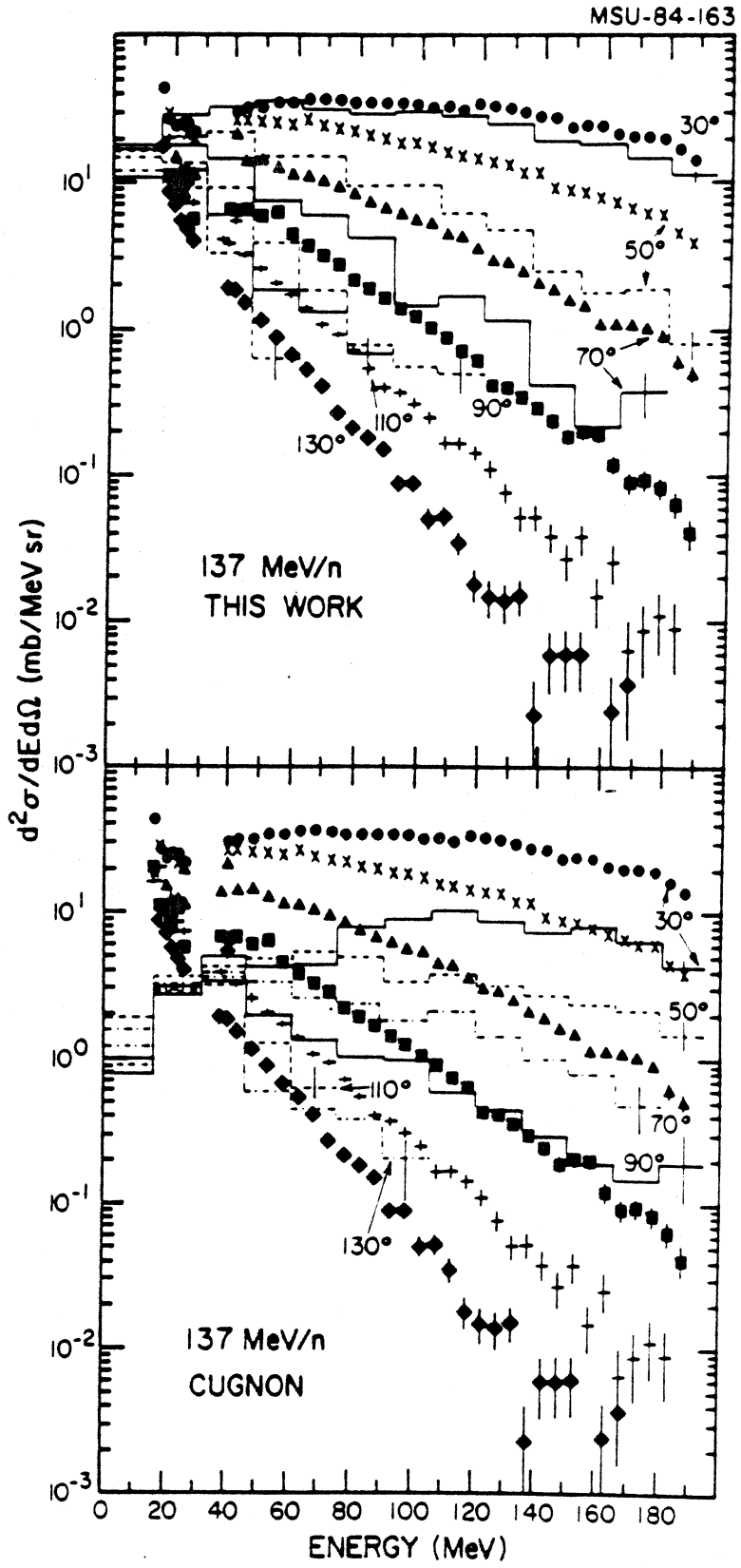
MSU-84-163
30°
50°
70°
90°
110°
130°
137 MeV/n
THIS WORK
137 MeV/n
CUGNON
$d^2\sigma/dEd\Omega$ (mb/MeV sr)
ENERGY (MeV)

Fig. 4

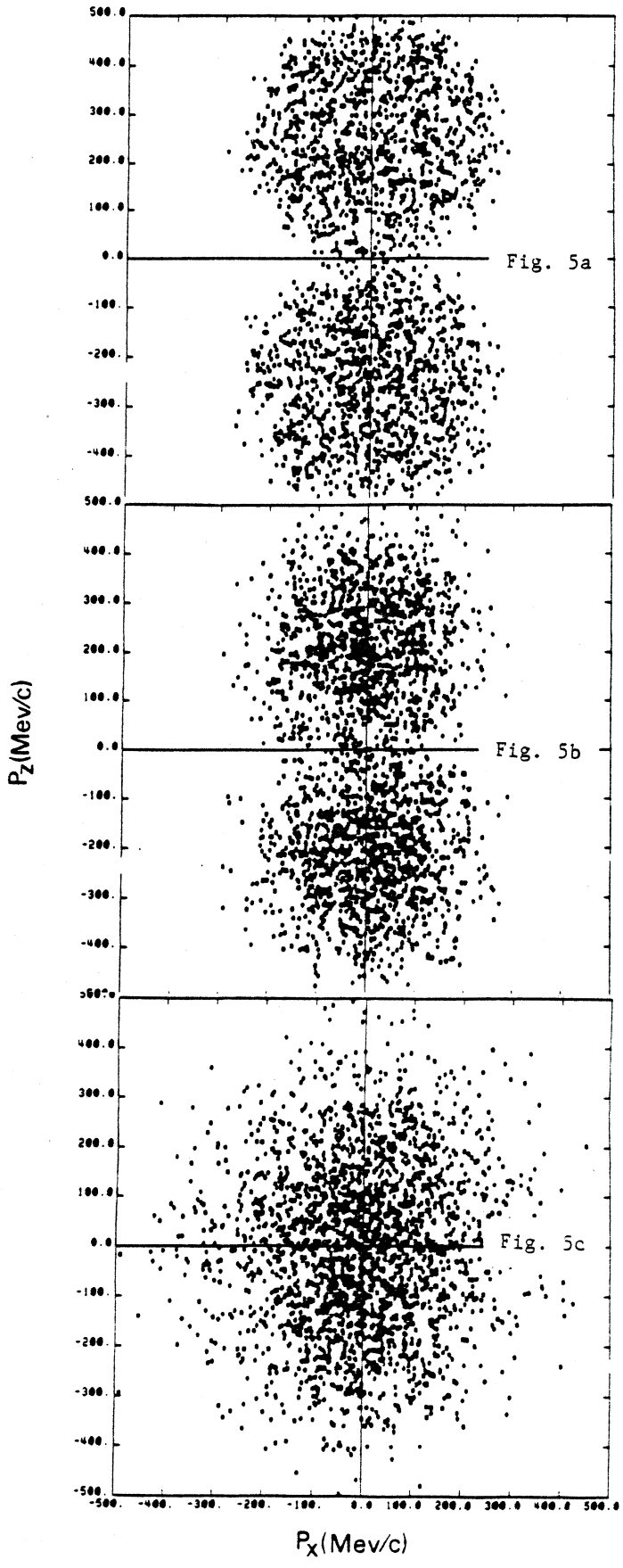
Fig. 5a
Fig. 5b
Fig. 5c
P_z(Mev/c)
P_x(Mev/c)

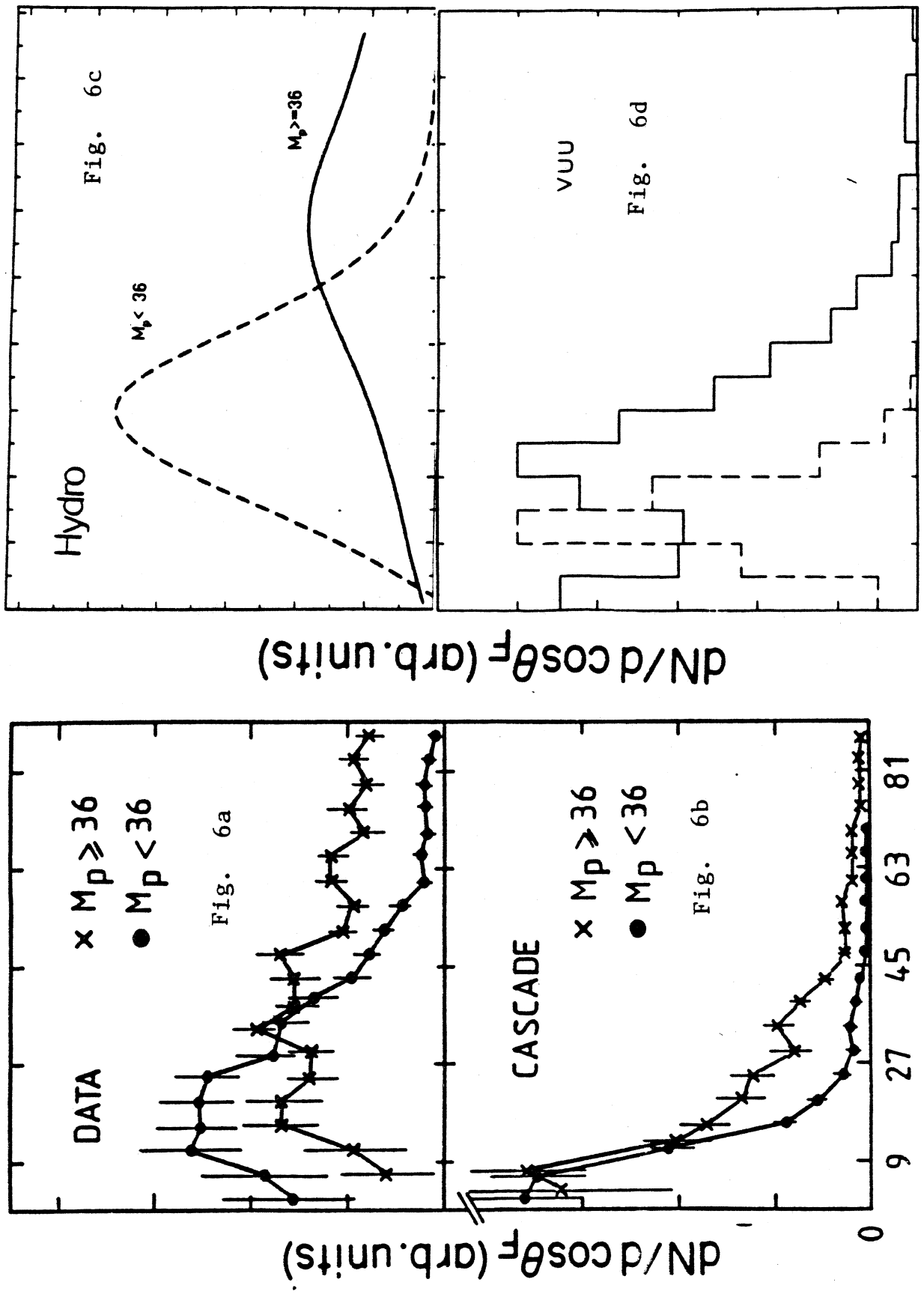
Ar + Pb, 0.77 GeV/u
DATA
× $M_p \geq 36$
● $M_p < 36$
Fig. 6a
CASCADE
× $M_p \geq 36$
● $M_p < 36$
Fig. 6b
Hydro
$M_p < 36$
$M_p \geq 36$
Fig. 6c
VUU
Fig. 6d
$dN/d\cos\theta_T$ (arb. units)
$dN/d\cos\theta_T$ (arb. units)
0
9
27
45
63
81
20
40
60
80
THETA (DEGREES)

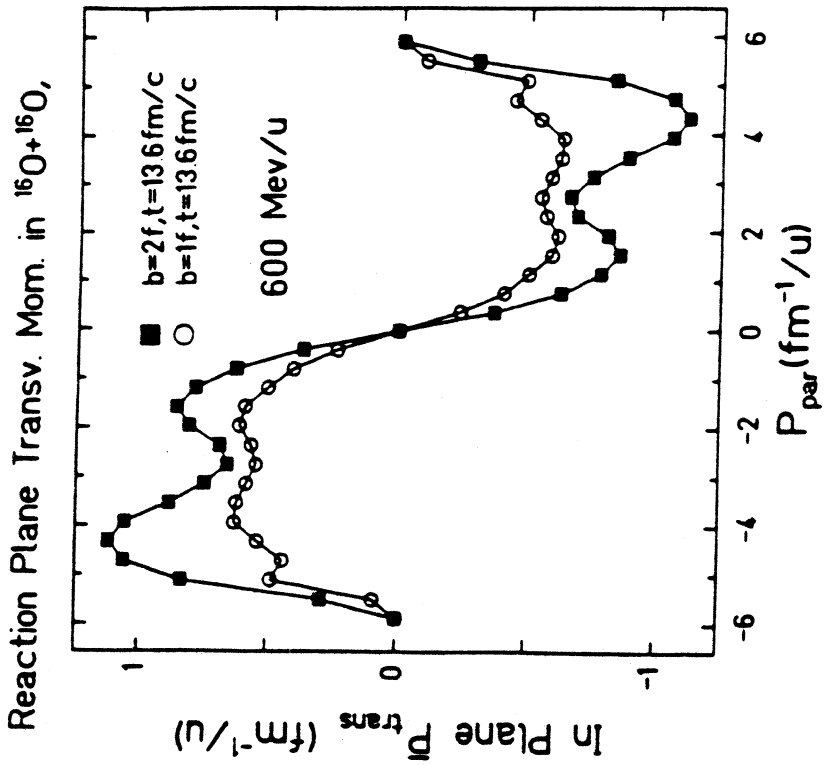
Reaction Plane Transv. Mom. in $^{16}O+^{16}O$,
600 Mev/u
b=2f,t=13.6fm/c
b=1f,t=13.6fm/c
In Plane P_{trans} (fm^{-1}/u)
$P_{par}(fm^{-1}/u)$

Fig. 8

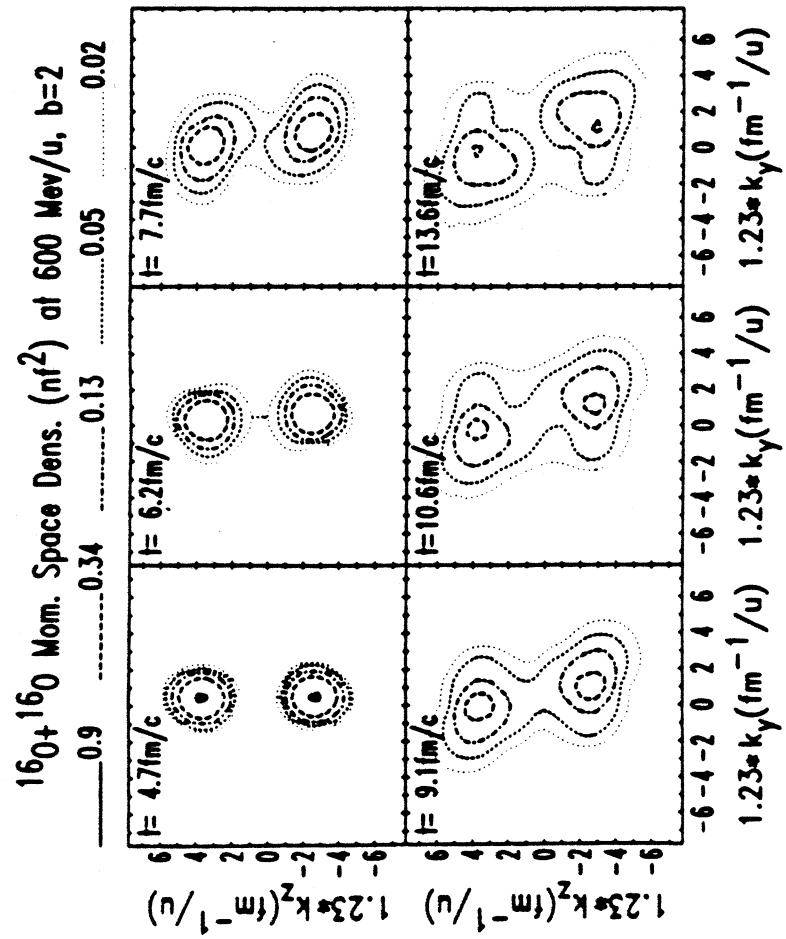
$^{16}O+^{16}O$ Mom. Space Dens. (nf^2) at 600 Mev/u, b=2
0.9
0.34
0.13
0.05
0.02
t= 4.7fm/c
t= 6.2fm/c
t= 7.7fm/c
t= 9.1fm/c
t=10.6fm/c
t=13.6fm/c
$1.23*k_z(fm^{-1}/u)$
$1.23*k_y(fm^{-1}/u)$

Fig. 7

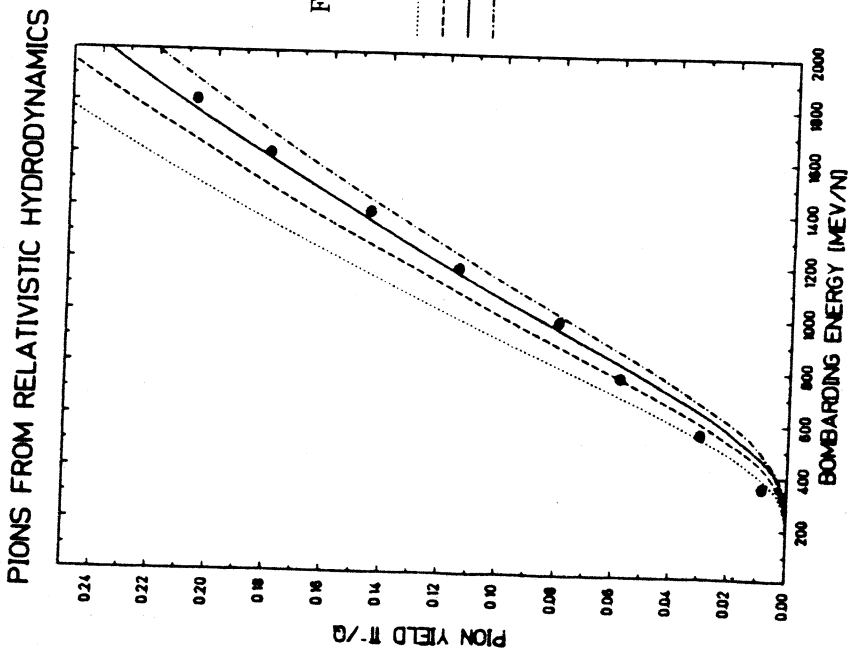
PIONS FROM RELATIVISTIC HYDRODYNAMICS
DATA GSI/LBL
K=100 MEV
K=200 MEV
K=300 MEV
K=400 MEV
QUAD EOS
PION YIELD π⁻/A
BOMBARDING ENERGY (MEV/N)

Fig. 10

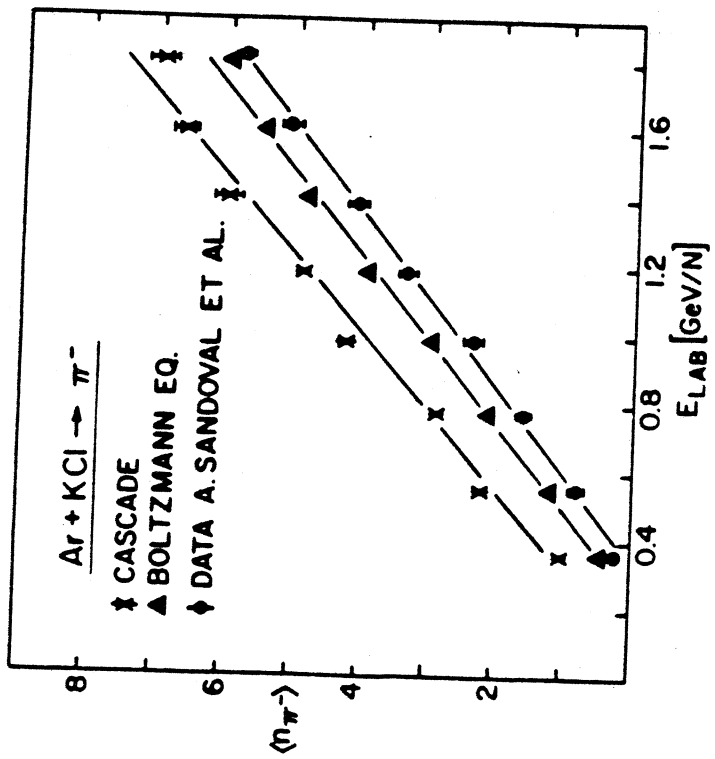
Ar + KCl → π⁻
CASCADE
BOLTZMANN EQ.
DATA A.SANDOVAL ET AL.
⟨nπ⁻⟩
E_LAB [GeV/N]

Fig. 9

The increase in deuteron production with increasing multiplicity can be described by the coalescence model taking into account both the size of the deuteron and the the volume of the participant region.[8]

The analysis of the Nb(400 MeV/N)+Nb data shows approximately the same cluster production as in 400 MeV/N Ca+Ca at the same multiplicity number of participants. Furthermore, a comparison of the cluster production at different bombarding energies but fixed number of participants yields a decrease of R_{dp} with increasing energy.[8] Hence, the asymptotic (extracted to infinite multiplicity) "d" to "p" values may be used to extract the entropy. Fig. 11 shows the entropy as a function of the bombarding energy calculated in the hydrodynamic model for a stiff Walecka and a soft Boguta equation of state. The entropy values as extracted from the asymptotic value of d/p observed for Nb+Nb at 400, 650 MeV and Ca+Ca at 1050 MeV/u are shown for comparison.[8] The data seem to indicate a rather stiff nuclear equation of state in qualtitative agreement with the results from pion production and collective flow.

7. Deconfinement in the Baryon Rich Region

Conjectures that a quark-gluon plasma can be formed in central nuclear collisions at energies $E_{Lab} > 1$ GeV/N rely on the extrapolation from experimental observations at higher energy proton- proton and lower energy nucleus- nucleus collisions. The former data indicate that the mid rapidity region has net baryon numbers close to zero.[24,25] Hence, if nucleons in nuclei behave like free nucleons, nuclei should become transparent at high energies and a clear kinematic separation between the baryon rich fragmentation regions of projectile and target is expected.[26,27] In the few GeV/N bombarding energy range, on the other hand, nuclear stopping has been observed.

Recent calculations based on the inside out cascade yield a strong leakage of baryons into the midrapidity region.[28] Baryon number densities as high as 2/3 of normal nuclear matter density are obtained at mid rapidity; even higher densities are predicted at rapidities closer to the projectile and target.

Hence we may be forced to infer that a zero chemical potential plasma cannot be formed in nuclear collisions at energies as high as E_{lab}=100 GeV/N. Then one would have to deal with a baryon rich plasma at all rapidity values. Unfortunately, theoretical information about the high density (high chemical potential) behaviour of QCD matter is very limited. Lattice QCD calculations of the thermodynamic properties of a plasma containing light quarks are hampered by severe theoretical difficulties: the introduction of fermions on the lattice is at this time only feasible in the quenched approximation.[29] The situation of interest here, a plasma of light quarks and antiquarks plus gluons, can therefore not be studied to date.

The thermodynamic properties of a plasma of light quarks and gluons at finite μ and T may be roughly inferred from perturbative QCD,[30-33] but sizable nonperturbative corrections must be made. In the bag model, the thermodynamical potential of a finite temperature plasma at nonzero chemical potential has been calculated up to third order[32] in α

$$-\Omega = P = \frac{8\pi^2}{45} T^4 + \frac{7\pi^2}{60} n_f T^4 +$$

$$n_f\left(\frac{1}{4\pi^2} \mu^4 + \frac{1}{2} T^2\mu^2\right) - g^2\left(\frac{T^4}{6} + \frac{5n_f T^4}{72} + \frac{1}{8} n_f\left(\frac{\mu^4}{\pi^4} + \frac{2\mu^2 T^2}{\pi^2}\right)\right)$$

This expression agrees to within a few percent with the correct result. This theory therefore has two free parameters, namely the scale fixing parameter Λ_{MOM} and the energy density of the real vacuum Λ_{VAC}. Λ_{MOM} and Λ_{VAC} can be determined by adjusting the pressure and energy density calculated in this approach at zero chemical potential to SU(N) Yang Mills Monte Carlo data. One obtains[34] Λ_{MOM}=100 MeV and Λ_{VAC}=190 MeV/fm^{-3}. The energy density e, entropy density s, and baryon number ρ of the deconfined quark gluon phase are obtained from the thermodynamical potential via

$$e = -\mu \frac{\partial \Omega}{\partial \mu} - T \frac{\partial \Omega}{\partial T} + \Omega, \quad s = -\frac{\partial \Omega}{\partial T}, \quad \rho = -\frac{1}{3} \frac{\partial \Omega}{\partial \mu}$$

Quark matter is apparently energetically disfavoured compared to ordinary nuclear matter: the minimum energy per baryon of the deconfined phase is about 1.34 GeV, for Λ_{MOM}=100 MeV and Λ_{VAC}=190 MeV/fm^3. Only at densities $\rho > 8\ \rho_0$ would the deconfined state be energetically favorable compared to confined matter at the same density. The energy per particle depends on the choice of Λ_{VAC} and Λ_{MOM}. The energy gap is 0.9 GeV/N when Λ_{VAC} is increased to 450 MeV/ fm^3. The energy density at the crossing of the two equations of state is 0.8 - 2.2 GeV/fm^3, hence in the same bulk part as the critical energy density obtained from Monte Carlo data at μ=0.

A first order phase transition can be constructed from the quark- and the hadron phase calculations by equating the pressures of the two phases at the same chemical potential and temperature.[35] The resulting phase coexistence regions are shown in Fig. 12. Observe the rather small gap in the density- temperature plane, in contrast to the wide coexistence regime in the energy density Fig. 14.

To get a rough estimate of the energy density achievable in a nucleus nucleus collision, let us in the following assume[36] that hydrodynamics is valid at higher energies, E_{lab} > 1 GeV/N. This extrapolation is questionable at very high energies, E_{lab} > 20 GeV/N, because of the longitudinal growth which may lead to the 'transparency'.[24,25,37] In the hydrodynamic calculations, the energy densities attainable depend on the equation of state (EOS) used; see fig. 15. The 'critical' energy densities, e = 1 - 2 GeV/fm³, may be reached at E_{lab}^{crit} = 4-7 GeV/N, values surprisingly modest compared to the values E_{lab} > 100 GeV/N considered to be necessary to form the baryon free plasma.

Graebner et al. have studied the space- time evolution of the zone of highest energy density in the hydrodynamic model;[13] see fig. 16. It is found that with light projectiles high energy densities are achieved only for times ~ 3 fm/c and only for a rather small number of nucleons (10 - 20) even when heavy target nuclei are used. In particular, the AGS beams (A < 30) may even in the optimistic scenario, assuming complete hydrodynamic stopping, not even result in energy densities of 2 GeV/N, while with a lead beam of only 5 GeV/N, this critical energy density may well be achieved for as many as 200 participating baryons.

The dynamical path of a collision in the ρ-T plane, the phase diagram of hadronic matter, as obtained from a simplified one dimensional treatment of the reaction is depicted in Fig. 13. The initial stage of high compression and excitation is followed quickly by the isentropic expansion of the system. The matter cools only modestly during the dense stage where baryon densities exceed normal nuclear density. At densities below normal density, the system is cooled much more rapidly due to the formation of pions. Also shown in the figure are contours of constant energy densities

of 1 and 1.5 GeV/fm³ of the deconfined phase. Observe that according to the present calculation bombarding energies E_{lab} > 2-4 GeV/N could be sufficient for deconfinement to occur in stopping collisions; see fig. 15. If deconfinement actually would occur at these rather modest energies, the energy gap between confined and deconfined matter would result in temperatures and entropies substantially lower than those calculated under the assumption that deconfinement does not happen. Fig. 17 shows the entropies[38] calculated in the hydrodynamic model assuming that deconfinement i) does and ii) does not occur. The plasma equation of state is used to calculate i) and Walecka's relativistic mean field equation of state is used for ii). The nuclear matter entropy exceeds 4 at E_{lab} > 2 GeV/N. The plasma entropy, on the other hand, is zero at the critical energy necessary to overcome the energy gap, E_{crit} = 2.2 and 4.2 GeV/N for Λ_{VAC}= 190 and 450 MeV/fm³, respectively. This mechanism of 'cold' plasma production has been discussed previously.[36-39]

It should be noted that none of the discussed possible experimental signatures for the deconfinement transition (dilepton-,[40] photon-,[41] strangeness[42] production) could work in this baryon rich region: these signatures rely on the very high temperatures predicted for the baryon free plasma, while at the same energy density the temperatures in the baryon rich plasma are much lower. Another signature pointed out recently is the production of anti-nuclei.[35]

The plasma entropy increases very fast with the the bombarding energy as compared to the nuclear matter curve. This is due to the repulsive interaction in nuclear matter, in particular in Walecka's model, to be contrasted with the quark-gluon plasma which tends towards asymptotic freedom, i.e. less interactions, with increasing energy density. Hence, the

entropy of the plasma phase would exceed the entropy of the confined phase after a transition domain in bombarding energy of about 2 GeV/N. The measurement of the entropy would thus provide an excellent signature for the onset of the deconfinement transition. It could also be very useful for plasma diagnostics because of it's sensitivity to the interactions.

A significant amount of entropy is produced in the condensation discontinuity, which develops at the transition from the quark phase into the hadron phase. It stems from the latent heat (excitation energy) released when the gap energy (0.4 to 0.9 GeV/N) is set free upon recondensation.[38] Some part of the internal energy available is thereby transformed into kinetic energy of the material which is formed behind the condensation discontinuity. The calculated entropy after condensation is depicted in Fig. 11e. Observe the large jump from almost zero entropy in the deconfined phase just above the critical bombarding energy to S/A > 7 after recondensation. This increase in fact depends on the vacuum pressure and on the momentum cut off, hence it may be useful for plasma diagnostics. Naturally this threshold increase of S/A would serve as a unique signature for the deconfinement transition. In contrast to the signatures discussed previously, which all rely on the formation of a baryon poor high temperature plasma, this signature does not depend on getting information out of the primordial plasma state before it recondensates but it rather uses the unusual properties of the recondensed matter after the short lived initial state has decayed.

9) Y. Yariv and Z. Fraenkel, Phys. Rev. C20, 2227 (1979); C24, 488 (1981);
V.D. Toneev, K.K. Gudima, Nucl. Phys. A400, 173 (1983).
J. Cugnon, D. Kinet, J. Vandermeulen, Nucl. Phys. A379, 553 (1982);
J. Cugnon, T. Mituzani, J. Vandermeulen, Nucl. Phys. A352, 505 (1981).

10) J.J. Molitoris, J.B. Hoffer, H. Kruse, H. Stöcker, Phys. Rev. Lett. 53, 899 (1984)
J.J. Molitoris, H. Stöcker, to be submitted to Phys. Rev. C.

11) A.R. Bodmer, C.N. Panos, Phys. Rev. C15 (1977) 1342;
A.R. Bodmer, C.N. Panos, A.D. MacKellar, Phys. Rev. C22, 1025 (1980);
A.R. Bodmer, C.N. Panos, Nucl. Phys. A356, 517 (1981).
A.R. Bodmer, Proc. 5th High Energy Heavy Ion Study, May 1981, p. 648, LBL-12652, Berkeley, California.

12) L. Wilets, E.M. Henley, M. Kraft, A.D. MacKellar, Nucl. Phys. A282 (1977) 341; L. Wilets, Y. Yariv, R. Chestnut, ibid. A301, 359 (1978);
D.J.E. Callaway, L. Wilets, Y. Yariv, ibid. A327, 250 (1979).

13) G. Buchwald, G. Graebner, J. Theis, J. Maruhn, W. Greiner, and H. Stöcker, Phys. Rev. Lett., 52, 18 (1984).
G. Graebner, et al., to be published.

14) H. Kruse, B. Jacak, H. Stöcker Phys. Rev. Lett. in press.

15) P. Danielewicz and M. Gyulassy, Phys. Lett. 129B, 283 (1983).

16) G. Bertsch, H. Kruse, and S. Das Gupta, Phys. Rev. C29, 673 (1984).

17) H. Kruse, B. Jacak, J.J. Molitoris, G.D. Westfall, H. Stöcker, submitted to Physics Letters.

18) S. Nagamiya, M.C. Lemaire, E. Moeller, S. Schnetzer, G. Shapiro, H. Steiner, I. Tanihata, Phys. Rev. C24 (1981) 971;
B. Jacak, G.D. Westfall, C.K. Gelbke, L.H. Harwood, W.G. Lynch, D.K. Scott, H. Stöcker, M.B. Tsang, T.J.M. Symons,

to be published;

U. Heinz, P.R. Subramanian, W. Greiner, Z. Physik, in print.

36) H. Stöcker, G.F. Graebner, J.A. Maruhn, W. Greiner, Phys. Lett. 95B (1980)192.

37) M. Gyulassy, LBL preprint 16292 (1983).

38) H. Stocker, Nucl. Phys. A 418 587 (1984).

39) T.S. Biro, J. Zimanyi, Nucl. Phys. A395 (1983) 25.

40) G. Domokos, J. Goldman, Phys. Rev. D23 (1981) 203.

41) K. Kajantie, H.I. Mietinnen, Z. Physik C9 (1981) 341, and C14 (1982) 357.

42) P.Koch, J. Rafelski, W. Greiner, Phys. Lett. 123B (1983) 151;

T.S. Biro, J. Zimanyi, Phys. Lett. 113B (1982) 6;

J. Rafelski, B. Muller, Phys. Rev. Lett. 48 (1982) 1066.